Nano Today 38 (2021) 101186

Contents lists available at ScienceDirect

Nano Today

journal homepage: www.elsevier.com/locate/nanotoday

Shear force responsive and fixed-point separated system for targeted treatment of arterial thrombus

Huijuan Zhang[a,b,c], Yamin Pei[a], Linyu Gao[a], Qingqing He[a], Hongling Zhang[a], Ling Zhu[a,b,c,*], Zhenzhong Zhang[a,b,c,*], Lin Hou[a,b,c,*]

[a] School of Pharmaceutical Sciences, Zhengzhou University, Zhengzhou, China
[b] Key Laboratory of Targeting Therapy and Diagnosis for Critical Diseases, Henan Province, China
[c] Collaborative Innovation Center of New Drug Research and Safety Evaluation, Zhengzhou, Henan Province, China

ARTICLE INFO

Article history:
Received 29 January 2021
Received in revised form 23 April 2021
Accepted 6 May 2021
Available online 26 May 2021

Keywords:
Thrombus targeting
Shear force response
Fixed-point separated
Sequential drug release
Combined attack and defense therapy

ABSTRACT

Thrombolytic treatment is the primary method for thrombotic diseases. However, uncontrollable bleeding and secondary vascular embolism are prone. Based on the thrombus microenvironment, this project constructed an "on-off " drug depot that can accurately identify thrombus and respond to changes of shear force to solve above problems. The fucoidan (Fuc)-based core-shell NPs were prepared by β-CD host-guest inclusion interaction. The thrombolytic drug urokinase (UK) and antiplatelet drug tirofiban (TI) were loaded into outer shell and inner core, respectively. In vitro and in vivo results proved that UK@Fuc-TI/PPCD was closed under low blood shear force to reduce bleeding risk. Once arriving at thrombus site, UK@Fuc-TI/PPCD can realize precise “homing” by recognizing P-selectin overexpressed by thrombus. Then sharply increased shear force at targeted thrombus broke the core-shell structure to release UK rapidly, realizing site-specific thrombolysis. Subsequently, TI loaded in PPCD core was slowly released at thrombolysis site, preventing re-embolization of blood vessels. Thrombolysis results demonstrated the in vitro thrombolysis rate of UK@Fuc-TI/PPCD pre-treated with 1000 dyne/cm^2 shear force was 91.59%. And in vivo, the percentage of residual thrombus in UK@Fuc-TI/PPCD treatment group was only 9.37% with relatively low bleeding risk, suggested this shear fore-responsive detachable system with thrombus targeting ability and sequential drug release profile can realize the efficient recanalization of embolized vessels.

Introduction

The consequences of arterial thrombosis are often fatal. Its formation can lead to vascular obstruction or complete occlusion, and then cause major events such as ischemic stroke and acute myocardial infarction. At present, the number of deaths due to acute cardiovascular and cerebrovascular diseases induced by arterial thrombosis each year has exceeded that of tumors, becoming the "first killer" that endangers human health [1]. Rapid removal of clots to restore blood supply is the key to treat these diseases. Common clinical treatment methods include drug therapy, interventional therapy and surgical treatment. However, since interventional and surgical therapy are invasive treatment methods and easily restricted by the embolization position, drug thrombolysis is still the most universal used method [2,3]. Among all thrombolytic agents, plasminogen activator (such as streptokinase, urokinase, alteplase, etc.) is the most commonly used. It activates the endogenous fibrinolytic system and degrades fibrinogen and coagulation factors (V and VIII, etc.), to exert a thrombolytic effect. However, these drugs have some shortcomings: (1) Due to lack of specificity, thrombolysis efficiency is reduced; (2) Because of the wide range of action sites, it is easy to cause serious uncontrollable bleeding risk (such as intracranial hemorrhage) [3]; (3) After thrombolysis, the local blood vessels are in a hypercoagulable state. Activated platelets are likely to re-aggregate to form new platelet thrombi, leading to re-embolization of blood vessels (occurrence rate ~25–30%) and greatly reducing thrombolysis effect [4].

To achieve specific delivery and controllable release of thrombolytic drugs in the local thrombus, reduce the risk of systemic bleeding, and prevent re-aggregation of platelets after thrombolysis, is an important topic that needs to be resolved. The Nano Drug Delivery System (NDDS), which is based on improving the distribution, metabolism, release and other behaviors of drugs in the

* Corresponding authors at: School of Pharmaceutical Sciences, Zhengzhou University, Zhengzhou, China.
E-mail addresses: zhuling1975@zzu.edu.cn (L. Zhu), zhangzz08@126.com (Z. Zhang), houlin_pharm@163.com (L. Hou).

https://doi.org/10.1016/j.nantod.2021.101186
1748-0132/

body, can create a unique approach from pharmaceutics and provide new strategies for solving this clinical need [5–7].Studies have found that the pathological microenvironment of thrombus has important physical changes, that is, the blood shear force at the thrombus site increases sharply. The shear force of blood flow in normal arteries is 10–70 dyne/cm^2, while the shear force at the stenosis of blood vessels caused by thrombus can reach > 1000 dyne/cm^2 [8,9]. When more than 75% of coronary artery blockage, local shear force at thrombus is increased 53-fold [8]. The thrombotic microenvironment-activated NDDS constructed based on this feature can enhance the thrombolytic effect and reduce bleeding risk by realizing the local release of thrombolytic drugs at the thrombus site. Netanel et al. proposed for the first time that the high shear force at thrombus site can be used to achieve specific delivery of thrombolytic drugs, and constructed a shear-sensitive tPA-NPs NDDS. It can disintegrate in 10 min under high shear force, to release tPA at targeted thrombus, which can effectively reduce the area of pulmonary embolism (< 60%) [5]. Molloy [10] and Margaret [11] et al. used phospholipids and choline diphosphate (Pad-PC-Pad) to prepare shear-sensitive nanocapsules and lens vesicles, respectively. The amount of drug released at thrombus is ~6 times that of normal blood vessels.

Beta-cyclodextrin (β-CD) can form the supramolecular self-assembly system with a variety of guest molecules by the host-guest inclusion interaction, which owns a very sensitive shear response performance [12,13]. Kaplan and other studies have shown that when the shear force is increased by 10 times, β-CD self-assembled supramolecular system can realize the rapid release of biological macromolecules, which can be used for the controllable delivery of enzyme and antibody drugs [14]. Targeted delivery is a prerequisite for achieving controlled drug release at the specific site. Thrombus contains a large number of activated platelets, which can highly express P-selectin. Therefore, P-selectin can be used as a specific target for thrombus [15,16]. Studies have proved that fucoidan (Fuc) can mimic P-selectin glycoprotein ligand 1 (PSGL-1) and exhibit a high affinity for P-selectin. NDDS modified with Fuc can efficiently target arterial thrombosis [17].

After thrombolysis with fibrinolytic drugs, the local blood vessels are in a hypercoagulable state, and the activated platelets are likely to re-aggregate to form new thrombi, leading to re-embolization of blood vessels. Giving local anti-platelet therapy in time after rapid thrombolysis can effectively prevent the re-aggregation of activated platelets at the thrombolytic site to improve the rate of vascular recanalization [18–21]. In addition, lectin-like oxidized low-density lipoprotein receptor 1 (LOX-1) is highly expressed on the surface of damaged vascular endothelial cells which exposed locally after thrombolysis. The small molecule peptide LSIPPKA screened from the phage peptide library by White et al. shows a high affinity for LOX-1 [22], which can anchor the nanoparticles to damaged blood vessels and achieve enrichment of antiplatelet drugs in the thrombolytic region.

Based on the above background, this project intended to design an offensive and defensive combined NDDS that can accurately identify thrombus and sequentially release drugs. This study prepared a new kind of core-shell nanoparticles (NPs). The Fuc shell and LSIPPKA modified poly lactic-co-glycolic acid (PLGA) core (PPCD) were self-assembled into NPs via the host-guest inclusion interaction of β-CD and adamantane (Ada). The antiplatelet drug tirofiban (TI) and thrombolytic drug urokinase (UK) were loaded in PPCD core and Fuc polymer shell, respectively. This dual-targeted NDDS with shear fore-responsive detachable feature can realize precise treatment of thrombus in the trinity of attack-prevention-protection. As shown in Fig. 1, this system had the following characteristics: (1) Reduce the risk of uncontrollable bleeding (protection). It can maintain stability during blood cruise (low shear force) and avoid the exposure of UK to non-targets. (2) At the thrombus site, sharply increased shear force destroyed the shell and released UK locally to trigger rapid thrombolysis (attack). (3) After the core-shell separation, TI/PPCD core accurately identified the thrombolytic location and colonized. With the degradation of PPCD, TI was slowly released to prevent blood vessel re-embolization after thrombolysis (prevention).

Materials and methods

Materials

PLGA (Mw = 15,000 Da) was obtained from Daigang Biotechnology Co., Ltd (Jinan, China). Mono(6-amino-6-deoxy)-β-cyclodextrin (EDA-CD) was bought from Zhiyuan Biotechnology Co., Ltd (Binzhou, China). LSIPPKA was synthesized by Shenggong Bioengineering Co., Ltd (Shanghai, China). 1-Adamantanecarbonyl Chloride was got from Ron reagent (Shanghai, China). Fuc was sourced from Jiejing Group Co., Ltd (Rizhao, China). UK was purchased from Mackline Reagent Co., Ltd

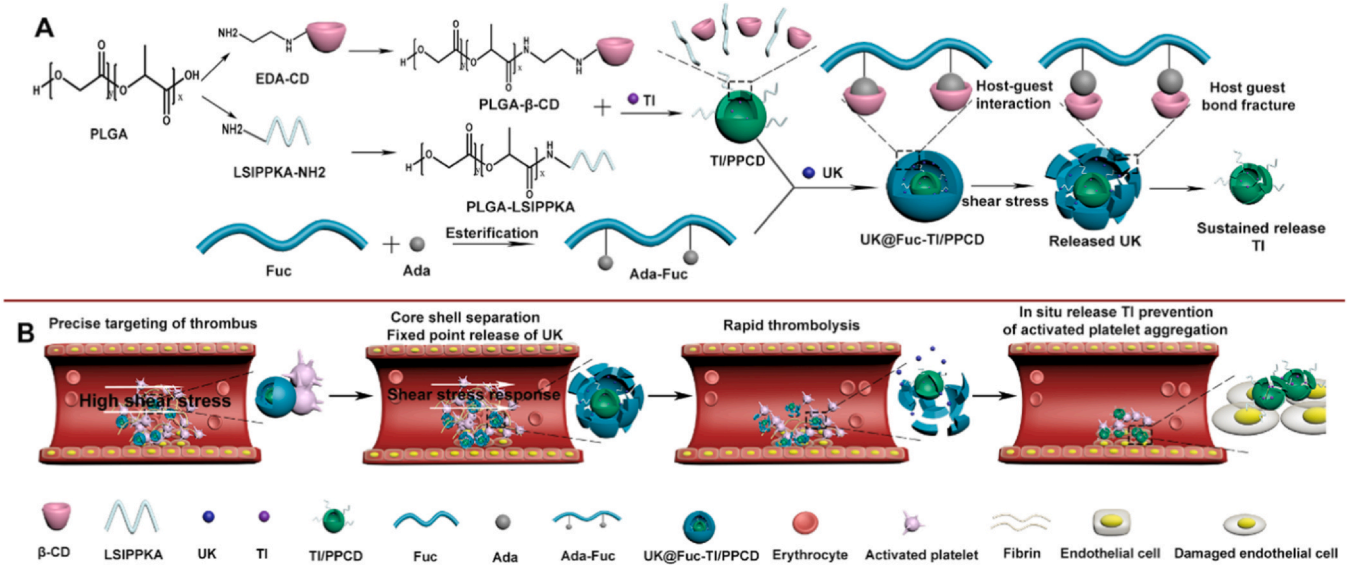

Fig. 1. Synthesis route and thrombolytic mechanism. (A) The synthesis route and drug release mechanism of UK@Fuc-TI/PPCD; (B) Schematic diagram of in vivo targeting thrombolysis of UK@Fuc-TI/PPCD.

(Shanghai, China). TI was got from Yuanye Biotechnology Co., Ltd (Shanghai, China). Fluorescein isothiocyanate (FITC), EDC·HCl, NHS and Sulforhodamine B (SRB) were got from Sigma-Aldrich (St Louis, USA). Human von Willebrand factor Kit was purchased from Ruixin Biotechnology Co., Ltd (Quanzhou China). Live / dead cell staining kit was obtained from Best Biotechnology Co., Ltd (Shanghai, China).

Synthesis of TI/PPCD NPs

The synthesis of TI/PPCD NPs was based on the method reported in the literature [23,24]. Firstly, PLGA (30 mg), EDC·HCl (1.6 mg) and NHS (1.0 mg) were dissolved in N, N-dimethylformamide (DMF, 3 mL) under magnetic stirring to activate the carboxyl group of PLGA for 30 min. Thereafter, EDA-CD (4.7 mg) was added to the mixture and reacted for 72 h. The precipitate obtained by centrifugation (8000 rpm, 30 min) was washed three times with ultra-pure water, followed by dialyzing (MWCO = 14,000 Da) and lyophilizing to obtain PLGA-β-CD. Similarly, PLGA (30 mg) and LSIPPKA (9 mg) were added into DMF (3 mL), and then treated with the same method to obtain PLGA-LSIPPKA.

Finally, TI/PPCD NPs were prepared by nanoprecipitation method. PLGA-β-CD (7 mg) and PLGA-LSIPPKA (3 mg) were dissolved in acetone (1 mL) at the ratio of 7:3. TI was dissolved in a small amount of methanol. Thereafter, the above two solutions were mixed and ultrasonic dispersed for 5 min. Next, drop this mixture into the poloxamer 188 (F68, 1%, 5 mL) solution at a speed of 0.5 mL/min. After rotary evaporation at 30 °C for 30 min, the reaction solution was dialyzed (MWCO = 8000 Da) to remove free TI and lyophilized to obtain TI/PPCD NPs.

Synthesis of UK@Fuc-TI/PPCD NPs

The synthesis of Ada-Fuc was conducted according to a previous reported procedure [13]. Primarily, dissolve Fuc (30 mg) in formamide (3 mL), then add DMAP (5 mg), pyridine (30 μL) and 1-adamantanecarbonyl chloride (8 mg) into Fuc solution. The mixture was allowed to stir for 24 h at room temperature. Next, the product was separated by precipitation using 2-propanol. After dissolving the precipitate in a minimum amount of water, dialysis (MWCO = 1000 Da) against water was adopted to purify the product. Finally, Ada-Fuc was collected and stored for further use by lyophilization.

Then, Ada-Fuc and TI/PPCD were mixed in water and self-assembled into UK@Fuc-TI/PPCD NPs. Exactly, Ada-Fuc (20 mg) and TI/PPCD (2 mg) were dissolved into water (2 mL). The solution was stirred at room temperature for 24 h and then UK (1 mg) was added. After continuing to react for 24 h, the mixture was centrifuged to separate the precipitated NPs. Finally, UK@Fuc-TI/PPCD was freeze-dried for further use after washing.

Characterization of TI/PPCD and UK@Fuc-TI/PPCD NPs

The morphological feature of NPs was monitored by the transmission electron microscopy (TEM). The molecular structure was confirmed by Fourier transform infrared spectroscopy (FTIR) and nuclear magnetic resonance hydrogen spectrometer (^{1}H NMR). The particle size distribution and zeta potential of NPs were measured by ZS90 laser nanoparticle size analyzer.

Determination of drug loading and encapsulation efficiency

The loading efficiency of TI was determined by HPLC method [25]. Briefly, according to method 1.2.2, TI/PPCD with different feed ratios were synthesized. The feed ratios of PPCD to TI were 1:2, 1:1 and 2:1, respectively. Thereafter, TI/PPCD NPs were demulsified with the mobile phase of HPLC, and then the loaded TI was extracted into the mobile phase for detection.

Firstly, the maximum absorption wavelength of TI was obtained by UV–vis spectrophotometer [26] to confirm the detection wavelength of TI for HPLC method. Next, standard solutions of TI were prepared to draw standard curve (seen in the Supplementary Material). HPLC chromatography conditions were as follows: 225 nm as the detection wavelength, Waters Symmetry C18 (4.6 × 150 mm, 5 μm) as the chromatographic column, 0.01 mol/L KH_2PO_4 buffer (pH 2.30): acetonitrile = 70:30 as the mobile phase, and 1.0 mL/min as the flow rate. Finally, the encapsulation and loading efficiency of TI was calculated as follows:

$$\text{encapsulation efficiency } (\%) = W_{\text{Loaded TI}} / W_{\text{Total TI}} \times ;100\%$$

$$\text{loading efficiency } (\%) = W_{\text{Loaded TI}} / W_{\text{TI/PPCD}} \times 100\%$$

In addition, UK was determined by BCA protein quantitative kit. Briefly, according to method 1.2.3, UK@Fuc-TI/PPCD with different feed ratios were synthesized. The feed ratios of TI/PPCD to UK were 2:1, 1:1 and 1:2, respectively. After that, UK loaded in UK@Fuc-TI/PPCD was extracted into PBS solution by ultrasonic method. According to the instruction of BCA protein determination kit, the standard curve of BCA was drawn, and the concentration of UK in PBS was determined. Finally, the loading and encapsulation efficiency of UK were determined according to the follow formula:encapsulation efficiency $(\%) = W_{\text{Loaded UK}} / W_{\text{Total UK}} \times 100\%$

$$\text{loading efficiency } (\%) = W_{\text{Loaded UK}} / W_{\text{UK@Fuc-TI/PPCD}} \times 100\%$$

Drug release evaluation

According to the existing literature reports [11,27], this study chose stretched capillary as the in vitro vascular embolization model with 80% of the middle blockage (Fig. 3E). The shear forces of 10, 250, 500 and 1000 dyne/cm^2 were obtained by controlling the flow rate of solution with a micro injection pump instrument. The calculation formula of shear force is: $\tau = 4\mu Q/\pi r^3$, where τ is shear force, μ is fluid viscosity, q is fluid flow rate and r is pipe radius. Then, UK@Fuc-TI/PPCD suspension with appropriate concentration was prepared. After 20 min of shearing under four shear forces, the amount of UK released in the supernatant was determined and normalized relative to the highest shear level (1000 dyne/cm^2) value. At the same time, released TI in the supernatant was also determined using HPLC method. Finally, the morphology of NPs after shearing with 1000 dyne/cm^2 force was observed by TEM.

Furthermore, the sustained-release characteristic of TI/PPCD was studied by dialysis method. In short, 3 mL of TI/PPCD aqueous dispersion or free TI solution was sealed in the dialysis bag (MWCO = 3500 Da), then incubated in 12 mL of PBS buffer. The experiment was carried out in a shaker at 37 °C with a shaking speed of 100 rpm. At the predetermined time points, take out 2 mL of release medium and add corresponding fresh medium with the same volume. The absorbance of TI was determined by UV-Vis spectrophotometry at 225 nm. The concentration of TI was calculated according to the standard curve and then the cumulative drug release percentage can be calculated.

Cytotoxicity of PPCD and Fuc-PPCD nanocarriers to vascular endothelial cells

HUVEC cells were seeded in the 96-well plate at a density of 3×10^5 cells/well and cultured for 24 h. The old medium was discarded and drug-containing medium (PPCD and Fuc-PPCD) was added. The concentrations of NPs were set as 5, 10, 20, 50 and 100 μg/mL. After incubation for 24 or 48 h with 5% CO_2 at 37 °C, cell viability was measured by SRB method. In addition, cytotoxicity was

also visually evaluated by double staining of living and dead cells. HUVEC cells were seeded in 6-well plates at a density of 3×10^5 cells/well. After incubation for 24 h, cells were treated with PPCD and Fuc-PPCD, respectively. After incubation for another 24 h, cells were washed and then stained with Calcein-AM dye at 37 °C for 15 min, PI dye at 37 °C for 2 min. The living cells (green) and dead cells (red) were observed and photographed under a fluorescence microscope.

The effect of nanocarriers on secretion of von Willebrand factor (vWF) by endothelial cells

HUVEC cells (3×10^5 cells/well) were seeded in 6-well plates and incubated for 24 h. Then cells were treated with PPCD and Fuc-PPCD nanocarriers for 8 h, respectively. The concentrations of NPs were all set as 5, 10, 20, 50 and 100 μg/mL. After that, the culture medium was centrifuged at 1000 rpm for 2 min and the supernatant was collected to determine vWF. The expression level of vWF was detected by VWF enzyme-linked immunosorbent assay (ELISA) kit.

Blood compatibility of PPCD and Fuc-PPCD nanocarriers

The hemocompatibility was evaluated via testing the hemolytic effect of nanocarriers on erythrocyte. As the literature reported [28], if NPs cause hemolysis, the contents of erythrocyte will be leaked. And the degree of hemolysis can be judged by detecting the absorbance at 540 nm of supernatant after centrifugation [29]. Briefly, the rat blood was collected with an EDTA anticoagulant tube and then erythrocyte precipitation was obtained by centrifugation at 2500 rpm for 20 min. For the experimental groups, Fuc-PPCD or PPCD nanocarriers were firstly dispersed in the saline solution to prepare a series of suspensions (5, 10, 20, 50 and 100 μg/mL), and then 1 mL of the nanocarrier suspensions of different concentrations were added to the erythrocyte precipitation respectively. Meanwhile, 1 mL of the pure saline and water (pH = 7.0) were added to the erythrocyte precipitation as the negative and positive groups, respectively. The volume concentration of erythrocyte in all groups was 1%. After incubation for 4 h, the absorbance of supernatant at 540 nm was measured after centrifugation (15,000 rpm, 5 min).

The targeting ability of PPCD nanocore to damaged HUVEC cells

LOX-1 was highly expressed on the surface of damaged endothelial cells [22]. LSIPPKA, a small peptide has been proved a high affinity for LOX-1 [30]. In this study, flow cytometry was used to study the targeting effect of PPCD cores modified by LSIPPKA to damaged endothelial HUVEC cells. In brief, HUVEC cells were seeded in a 6-well plate at a density of 3×10^5 cells/well and then incubated for 24 h. Thereafter, cells were incubated in a medium containing 0.5 mM hydrogen peroxide (H_2O_2) for 2 h to induce endothelial cell damage. Next, the medium was replaced with FITC/PPCD-containing medium. The concentration of FITC was 15 μg/mL. After incubation for 0.5, 1, 2 and 4 h, cells were washed twice with PBS buffer and digested with trypsin. Finally, the cells were collected and re-suspended with 200 μL of PBS for detection using flow cytometry.

The targeting ability of Fuc-PPCD to activated platelet

HUVEC cells were seeded in 35 mm petri dishes (1.5×10^5 cells/dish) and cultured for 24 h. Then Calcein AM-labeled platelets (Supplementary Material) were added to these dishes. After activation with 0.1 μg of $CaCl_2$ and 1 IU of thrombin for 0.5 h, the inactivated platelets were gently removed by washing three times with PBS buffer. Next, Rhodamin B-labeled Fuc-PPCD or PPCD nanocarriers (Supplementary Material) were added to the dishes at a concentration of 50 μg/mL. After incubation at 37 °C for 2 h, excess NPs were removed by washing three times with PBS. The cells were fixed with 4% paraformaldehyde and the nucleus of HUVEC cells was stained with Hoechst 33342. Confocal microscopy was used to observed and recorded the co-localization of NPs and activated platelets.

In vitro blood clot preparation

Platelet-rich plasma (PRP) was prepared from sodium citrate anticoagulated whole blood collected from healthy rats [10]. The whole blood collected from rats was centrifuged at 1200 rpm for 20 min. After repeated centrifugation, the supernatant was taken as platelet-rich plasma. Mix this plasma with 10 μL of erythrocytes suspension. Then add 180 μL of the above plasma mixture in a 96-well plate. After that, add 5 U of thrombin and 5 mmol/L of $CaCl_2$ into the well and co-incubate in a shaker at 37 °C for 3 h to form blood clots.

In vitro thrombus targeting of NPs

The in vitro thrombus clots were prepared according to method 1.2.12. Then incubated them with saline, IR783, IR783@PPCD and IR783@Fuc-PPCD (Supplementary Material), respectively at 37 °C in a shaker. After 2 h of incubation, the supernatant was discarded and the clots were washed with saline. Then FX PRO optical intravital imager was used to record the results.

In vivo targeting study

Animals: SD female rats (180–200 g) were obtained from Henan Laboratory Animal Center (Henan, China). All animal procedures were performed in accordance with the Guidelines for Care and Use of Laboratory Animals of Drug Research Institute of Zhengzhou University (syxk 2018-0004).

Thrombus targeting of Fuc-PPCD core-shell nanocarriers in vivo: SD female rats were anesthetized with 10% chloral hydrate and both carotid arteries were exposed. A 2 × 3 mm filter paper immersed in 10% $FeCl_3$ for 1 min was placed on the right carotid artery for 8 min. After thrombus formation, IR783 labeled vector (Supplementary Material) was injected into tail vein immediately. The experiment was divided into IR783, IR783@PPCD and IR783@Fuc-PPCD groups. After 10 min of administration, the carotid arteries of rats were photographed using the FX PRO optical intravital imager and the fluorescence was quantitatively analyzed. What's more, for IR783@Fuc-PPCD group, the fluorescence accumulation in both sides of carotid arteries at different time points was observed (10 min, 30 min, 60 min, 90 min and 120 min).

Damaged endothelial cells targeting of PPCD cores in vivo: SD female rats were anesthetized with 10% chloral hydrate and both carotid arteries were exposed. Free UK was injected into caudal vein before 10% $FeCl_3$ injury. After a 2 × 3 mm filter paper immersed in 10% $FeCl_3$ was placed on the right carotid artery for 8 min, IR783-PPCD NPs were injected into tail vein immediately. And then the FX PRO optical intravital imager was used to record the results at different time points (10 min, 30 min, 60 min, 90 min and 120 min).

In vitro thrombolysis study

Prepare in vitro blood clots according to method 1.2.12. After that, clots of the same size were randomly divided into normal saline (N.S.), UK, TI, TI/PPCD, Fuc-PPCD, UK@Fuc-TI/PPCD and sheer stress UK@Fuc-TI/PPCD (Pre-treated in vitro with 1000 dyne/cm^2 shear force) groups. The dose of UK and TI were 40 and 8 μg/mL, respectively. The blood clots were incubated with the above preparations at 37 °C for different times (0 h, 1 h, 2 h, 3 h) to evaluate the in vitro thrombolysis effect. After the moisture was removed from the thrombus surface with filter paper, the weight of blood clots was

measured and recorded at different time points. Meanwhile, the weight ratio of blood clots at 3–0 h was calculated as thrombolytic rate.

In vivo thrombolysis study

SD female rats were randomly divided into following 8 groups: normal saline (N.S.) control, UK, TI, TI/PPCD, Fuc-PPCD, UK@Fuc-PPCD, UK@Fuc-TI/PPCD and Shear Stress UK@Fuc-TI/PPCD. Shear Stress UK@Fuc-TI/PPCD indicated that UK@Fuc-TI/PPCD was pre-sheared in vitro for 20 min under the shear force of 1000 dyne/cm^2. The dose of UK and TI was 1 mg/kg and 0.08 mg/kg, respectively. After SD rats were anesthetized with 10% chloral hydrate, the carotid artery on one side was exposed. The filter paper (2 × 3 mm) was immersed in 10% $FeCl_3$ solution and saturated for 1 min. Then, the paper was placed on the exposed carotid artery for 8 min o form local thrombus. Thereafter, different preparations were administered via the tail vein immediately. First, 10 min after administration, the tails of rats were cut off at 1 cm and then placed in N.S. solution to observe and record the tail bleeding time. Next, after 2 h of administration, carotid artery of the thrombus side was dissected out for H & E staining and the blood of rats was collected for coagulation index analysis.

Safety evaluation

Healthy SD rats were randomly divided into the following 4 groups: N.S., Fuc-PPCD, UK + TI and UK@Fuc-TI/PPCD. Drugs were intravenously injected into rats as a single dose. The rats were weighed every day for a total of 7 days. At the end of the experiment, the rats were sacrificed and major tissues (heart, liver, spleen, lung, kidney) were dissected immediately. All of the above tissues were made into paraffin sections to observe the pathological changes under a microscope after H&E staining. In addition, the blood samples were collected to measure liver function and kidney function indexes, ALT, AST, T-BIL and UREA.

Biodistribution

The biodistribution of IR783-labeled Fuc-PPCD (Supplementary Material) in the major organs (heart, spleen, lung, liver, and kidney) was investigated by FX PRO optical imager at pre-set time points (0, 2, 4, 6, 12 and 24 h). Briefly, healthy SD rats were randomly divided into 6 groups. IR783-labeled Fuc-PPCD was injected into caudal vein (the dose of IR783 was 1 mg/kg). Finally, the main organs of each group were dissected and photographed.

Statistical analysis

All data was analyzed using GraphPad Prism6 software (GraphPad Software, Diego, USA). One-way ANOVA was used for both multiple comparisons and a two-group comparison in multi-groups. **P < 0.05, **P < 0.01, and ***P < 0.001 were considered as statistically significant.*

Results and discussion

Characteristics of TI/PPCD NPs

Firstly, β-CD grafted PLGA (PLGA-β-CD) and LSIPPKA grafted PLGA (PLGA-LSIPPKA) were synthesized, respectively. PLGA-β-CD product was confirmed by FT-IR spectrum (Fig. 2A), with a newly generated -CO stretching vibration peak at 1759.73 cm^{-1}. The peak at 1625.23 cm−1 was attributed to the -NH bending vibration band. Meanwhile, the chemical structure of PLGA-β-CD was also investigated by 1H NMR (=Fig. 2B). The formants at δ 1.48 and 5.20 ppm were assigned to methyl and -CH groups of lactic acid (LA) repeating units, respectively. And the multiplets at δ 4.91 ppm were assigned

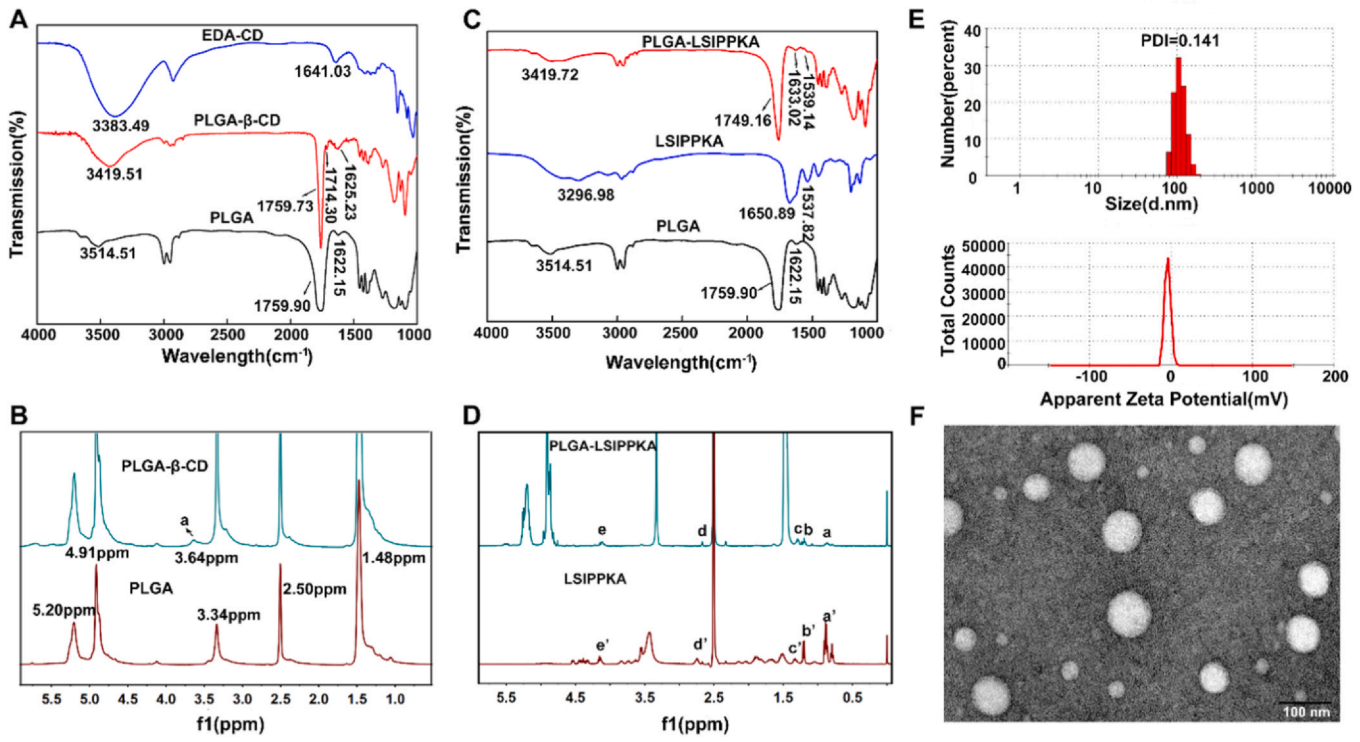

Fig. 2. Characteristics of TI/PPCD NPs. (A) FT-IR spectrum of PLGA, EDA-CD and PLGA-β-CD. (B) ^{1}H NMR spectrum of PLGA and PLGA-β-CD. (C) FT-IR spectrum of PLGA, LSIPPKA and PLGA-LSIPPKA. (D) ^{1}H NMR spectrum of LSIPPKA and PLGA-LSIPPKA (δ a: 0.91 ppm, δ b: 1.53 ppm. δ c: 1.67 ppm, δ d: 2.74 ppm and δ e: 4.15 ppm). (E) The particle size and zeta potential of TI/PPCD NPs. (F) TEM image of TI/PPCD NPs by negative staining technique.

to the methylene groups of GA residues, which confirmed the chemical structure of PLGA. The small peak at 3.64 ppm was attributed to the protons C_2–C6 of β-CD unit. Furthermore, the successful synthesis of PLGA-LSIPPKA was also confirmed by FT-IR and 1H NMR. As shown in Fig. 2C, 1633.02 cm−1 was the stretching vibration peak of carbonyl group and 1539.14 cm−1 was the bending vibration peak of N-H. In addition, the 1H NMR spectra further demonstrated the chemical structure of PLGA-LSIPPKA (Fig. 2D). The peaks at δ 0.91 (a), 1.53 (b), 1.67 (c), 2.74 (d) and 4.15 (e) ppm were assigned to the presence of LSIPPKA. The resonance peaks of PLGA-LSIPPKA appearing at δ 1.48, 5.20 and 4.91 ppm were consistent with that of PLGA spectrogram.

PPCD NPs were synthesized by nanoprecipitation method with PLGA-β-CD and PLGA-LSIPPKA at the ratio of 7:3. Meanwhile, TI was loaded into PPCD NPs to form TI/PPCD NPs. The maximum absorption wavelength of TI was 225 nm obtained by UV-Vis spectrophotometer (Fig. S1). The standard curve (Fig. S2) was established to determine the concentration of TI and optimize prescription conditions. As shown in Fig. S3, the optimal ratio of nanocarrier to TI was 2:1, with drug loading and encapsulation efficiency of 1.94% and 17.6%, respectively. The hydrodynamic diameter of TI/PPCD NPs was 111.7 nm with the polydispersity index (PDI) value of 0.141 (Figs. 2E and S4). And the zeta potential of TI/PPCD NPs was −4 mV. TEM image showed that TI/PPCD were spherical NPs with a uniform particle size distribution (Figs. 2F and S5).

Characteristics of UK@Fuc-TI/PPCD NPs

Firstly, Ada grafted Fuc (Ada-Fuc) was synthesized. As shown in Fig. 3A, the peaks of Ada-Fuc at 1729.89, 1258.89 and 1054 cm^{-1} were characteristic peaks of the formed ester bond, attributing to the stretching vibration peaks of -CO, C-O-C and C-O, respectively. The presence of Ada provoked a peak displacement of 2.02 ppm in the 1H NMR spectroscopy of Ada-Fuc, further proving that Ada was grafted on Fuc (Fig. 3B). After that, Fuc-TI/PPCD NPs were synthesized by the host-guest inclusion interaction between β-CD on TI/PPCD NPs and Ada on Ada-Fuc conjugate. Meanwhile, UK was selected as the thrombolytic drug and loaded in the outer shell of Fuc-TI/PPCD NPs to form the final UK@Fuc-TI/PPCD NDDS. As demonstrated in Figs. 3C and S6, the hydrodynamic diameter of UK@Fuc-TI/PPCD was 575.6 nm with PDI value of 0.387. Moreover, zeta potential result revealed that UK@Fuc-TI/PPCD was negative charged (−18 mV). In addition, as TEM image demonstrated

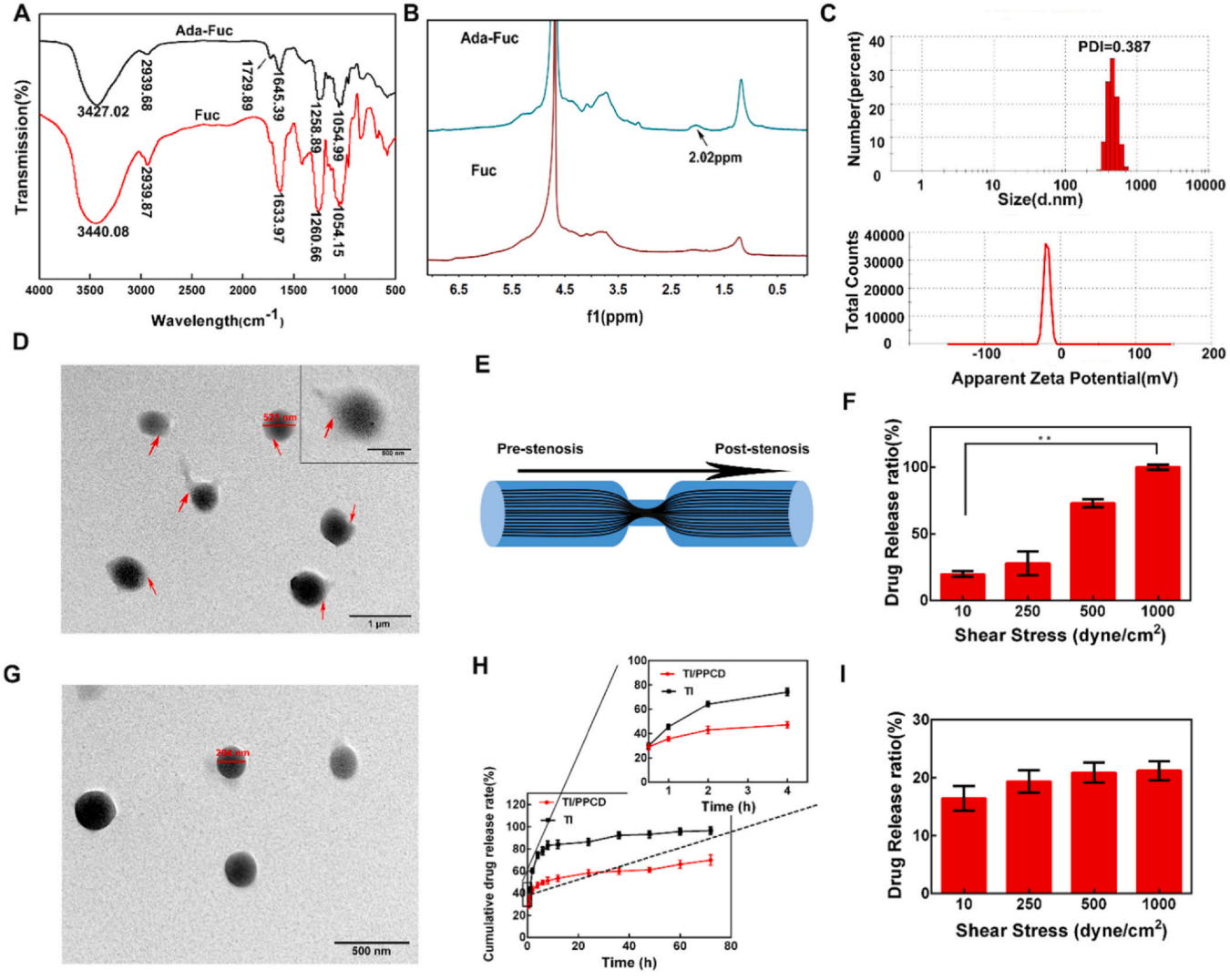

Fig. 3. Characteristics of UK@Fuc-TI/PPCD NPs. (A) FT-IR spectrum of Fuc and Ada-Fuc. (B) ^{1}H NMR spectrum of Fuc and Ada-Fuc. (C) The particle size and zeta potential of UK@Fuc-TI/PPCD NPs. (D) TEM image of UK@Fuc-TI/PPCD NPs. The shell was indicated by red arrow. (E) A self-made in vitro embolization model to simulate thrombus. (F) The shear force-responsive release curve of UK from UK@Fuc-TI/PPCD NPs for 20 min. Data is shown as mean ± SD (n = 3). (G) TEM image of UK@Fuc-TI/PPCD NPs after shearing (1000 dyne/cm^2) for 20 min (H) The sustained release profile of TI from TI/PPCD cores in PBS medium and free TI was used as the control. (I) The release profile of TI from UK@Fuc-TI/PPCD NPs under different shear forces for 20 min. Data is shown as mean ± SD (n = 3). $^{**}p < 0.01$.

(Fig. 3D), UK@Fuc-TI/PPCD NPs had a typical core-shell structure. The core and shell were composed of TI/PPCD NPs and UK loaded Ada-Fuc, respectively. Furthermore, the standard curve of UK was established using BCA protein kit to optimize prescription conditions (Fig. S7). As shown in Fig. S8, the optimal ratio of nanocarrier to UK was 2:1, with drug loading and encapsulation efficiency of 22.89% and 62.61%, respectively.

In vitro drug release profiles

The shear force-responsive release profile of UK was studied based on the method reported in the literature [27]. The in vitro embolism model was made by capillary, as shown in Fig. 3E. The released amount of UK was determined and normalized relative to the highest shear level (1000 dyne/cm$^{2)}$ value. As shown in Fig. 3F, the release profile demonstrated obvious shear force dependent characteristics. The cumulative released amount of UK at sheer force of 1000 dyne/cm^2 was 4.55 times more than that of 10 dyne/cm2. Furthermore, the morphological change of UK@Fuc-TI/PPCD NPs after shearing was verified by TEM. As seen in Fig. 3G, the Fuc shell layer on the surface of NPs had been removed and the particle size decreased from ~521 nm to ~204 nm, further proving the shear force sensitivity of UK@Fuc-TI/PPCD. As desired, after core-shell separation, TI/PPCD cores would be colonized at the thrombolytic site and slowly released TI to prevent re-aggregation of activated platelets. Therefore, the sustained-release profile of TI from TI/PPCD NPs was also investigated. As shown in Fig. 3H, compared with free TI, TI/PPCD NPs demonstrated obviously sustained release property. At 4 h, the cumulative drug release rate of TI in free TI and TI/PPCD groups were 74.29% and 47.22%, respectively. Meanwhile, the release profile of TI under different shear stress was also monitored to study the stability of TI/PPCD cores. As shown in Fig. 3I, there was no significant difference in the release of TI under various shear forces, proving the stability of TI/PPCD cores at thrombus site. All above results suggested that the sharply increased shear force at targeted thrombus could break core-shell structure of UK@Fuc-TI/PPCD to release UK rapidly, acting on the local fibrinolytic system to realize site-specific thrombolysis. Subsequently, TI loaded in TI/PPCD cores was slowly released at thrombolysis site, preventing re-embolization of blood vessels.

Cytotoxicity of PPCD and Fuc-PPCD nanocarriers

Cell compatibility is a prerequisite for the application of nanomaterials to thrombolytic therapy in vivo. Therefore, the cytotoxicity of PPCD and Fuc-PPCD nanocarriers to HUVEC cells was studied. As shown in Fig. 4A and B, the cell survival rates of HUVEC cells treated with PPCD or Fuc-PPCD NPs were all above 94%, even at a high

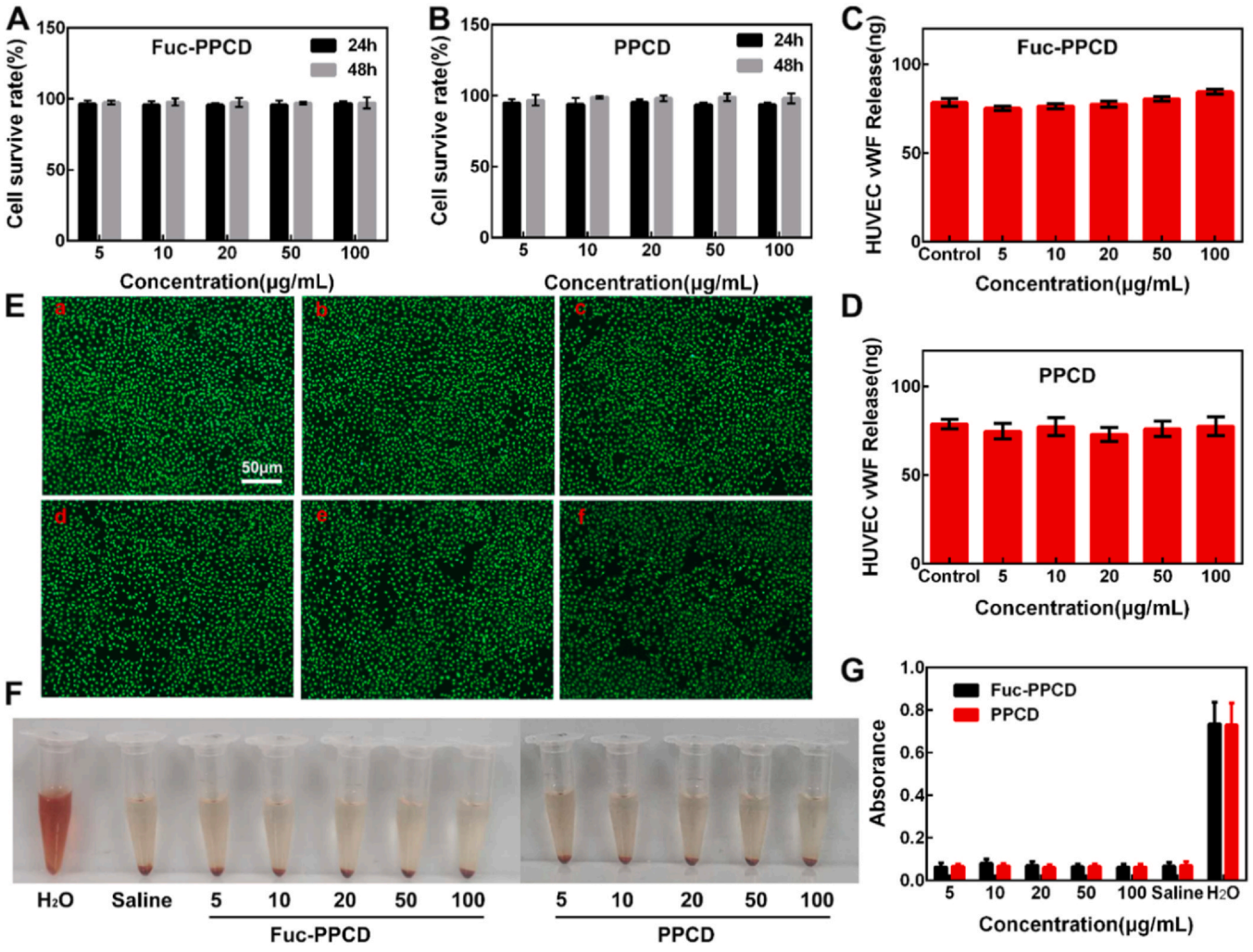

Fig. 4. Cytotoxicity and hemolysis of nanocarriers. (A) The cell survive rate of Fuc-PPCD on HUVEC cells for different time. (B) The cell survive rate of PPCD on HUVEC cells for different time. (C) The expression level of vWF in HUVEC cells incubated with different concentrations of Fuc-PPCD nanocarriers. (D) The expression level of vWF in HUVEC cells incubated with different concentrations of PPCD. (E) Live and dead cells staining result of Fuc-PPCD treated HUVEC cells by Calcein-AM/PI assay (a: control, b: 5 μg/mL, c: 10 μg/mL, d: 20 μg/mL, e: 50 μg/mL, f: 100 μg/mL). (F) The blood compatibility of Fuc-PPCD and PPCD nanocarriers with various concentrations. The unit was μg/mL. (G) The absorbance at 540 nm of blood samples incubated with various concentrations of Fuc-PPCD and PPCD nanocarriers. Saline and water were set as negative and positive control, respectively.

concentration of 100 μg/mL. What's more, the live/dead cell double staining result demonstrated there were no obvious dead cells appeared in the visual field after 24 h of treatment with PPCD and Fuc-PPCD nanocarriers (Figs. 4E and S9). All the above results proved that PPCD and Fuc-PPCD nanocarriers had good compatibility with HUVEC cells, which provided a prerequisite for their thrombolytic application in vivo.

Determination of vWF expression level

Von Willebrand factor (vWF) is a polymeric glycoprotein secreted mainly by vascular endothelial cells. The synthesis and release of vWF are closely related to the changes of internal and external environment of endothelial cells [31]. Therefore, we detected the expression level of vWF in endothelial cells to evaluate whether endothelial cells were damaged, so as to evaluate the cell safety of nanocarriers. ELSA kit was used to detect the expression of vWF in cells incubated with different concentrations of vectors. As shown in Fig. 4C and D, there was no significant difference in the expression of vWF by vascular endothelial cells incubated with different concentrations of PPCD and Fuc-PPCD nanocarriers. These results indicated that the nanocarriers will not cause damage to endothelial cells.

Blood compatibility

Blood compatibility is another prerequisite for the application of nanomaterials to thrombolytic therapy in vivo. If hemolysis occurs, hemoglobin will leak out of the red blood cells. Because hemoglobin has a maximum absorption at 540 nm, the hemolytic effect of NPs could be quantitatively evaluated by detecting the absorbance of samples at 540 nm (A540). As Fig. 4F and G shown, the hemolytic effect of PPCD and Fuc-PPCD nanocarriers on red blood cells was similar to that negative control group. The relatively low A540 value demonstrated that PPCD and Fuc-PPCD would not induce hemolytic effect in vivo and were safe for intravenous administration.

The targeted ability of PPCD cores to damaged HUVEC cells

After thrombolysis, damaged endothelial cells are exposed to blood vessels and the activated platelets are likely to re-aggregate to form new thrombi, leading to re-embolization of blood vessels. Therefore, in this study TI/PPCD cores was designed to targeted damaged endothelial cells via high affinity of LSIPPKA on the surface of TI/PPCD to LOX-1 receptor highly expressed by damaged vascular endothelial cells. Flow cytometry was used to evaluate the targeting ability of PPCD to damaged endothelial cells. PLGA NP without LSIPPKA modification was used as the control group. As Fig. 5A shown, compared with PLGA group, PPCD NPs demonstrated time-dependent targeted ability to damaged HUVEC cells. At 0.5, 1, 2 and 4 h, there was 26.1%, 39.5%, 67.4% and 73.8% of FITC labeled PPCD NPs accumulating in damaged HUVEC cells, respectively. Based on this result, we can know that after core-shell separation under high shear force at thrombus site, PPCD core accurately identified the thrombolytic location and colonized. And then TI was slowly released to prevent blood vessel re-embolization after thrombolysis.

The colocalization ability of Fuc-PPCD NPs with activated platelets

Activated platelet is the main component of thrombus, and can overexpress P-selectin. Studies had found Fuc can specifically bind to P-selectin that highly expressed on the surface of activated platelets [17]. Hence, the colocalization phenomena of Fuc-PPCD and activated platelets were visually studied to confirm the targeted ability of Fuc-PPCD by LSCM. Firstly, adherent HUVEC cells were co-incubated with activated platelets to simulate thrombosis in the vascular environment. Next, they were treated with Rhodamin B labeled Fuc-PPCD or PPCD NPs. As shown in Fig. 5B, Fuc-PPCD and activated platelets were almost completely overlapped with the colocalization coefficient of 0.879, suggested that Fuc-PPCD nanocarriers can specifically recognize and bind activated platelets in thrombus.

Thrombus targeting ability of Fuc-PPCD in vitro and in vivo

After labeled with IR783, the thrombus targeting ability of Fuc-PPCD nanocarriers in vitro and in vivo was evaluated by FX PRO optical imaging system (Kodak, USA). The fluorescence imaging result of in vitro thrombus clots after incubated with free IR783, IR783@PPCD and IR783@Fuc-PPCD was shown in Fig. 6A. The quantitative fluorescence statistics of various groups can be seen in Fig. 6B. The fluorescence intensity of thrombus clots treated with IR783@Fuc-PPCD NPs was the highest compared with that of the other two groups, indicated Fuc-PPCD nanocarriers had excellent thrombus targeting ability in vitro.

Meanwhile, the thrombus targeting effect of Fuc-PPCD was further studied in vivo. As shown in Fig. 6C and D, the fluorescence intensity of $FeCl_3$ pre-treated arteries in free IR783 group was low and similar to that of PPCD group at 10 min after administration. On the contrary, after injection of IR783@Fuc-PPCD for 10 min, the fluorescence intensity of FeCl3 pre-treated artery was much higher than that of the other two groups, while the fluorescence intensities of uninjured artery in IR783, IR783@ PPCD and IR783@Fuc-PPCD groups were similar. In addition, there was significant difference of fluorescence intensity between uninjured and injured arteries in IR783@Fuc-PPCD group. These results indicated that Fuc-PPCD also had good thrombus ability in vivo.

Furthermore, the real-time distribution of Fuc-PPCD in bilateral carotid arteries was monitored in vivo. As shown in Fig. 6E and F, Fuc-PPCD nanocarriers mainly accumulated in the injured vessel with thrombus after injection for 10 min. With the extension of time, the fluorescence intensity decreased, leaving only background fluorescence at 120 min. This was due to the shear fore responsive feature of Fuc-PPCD. After arriving at thrombus site existing in the injured vessel, increased shear force destroyed the core-shell structure of IR783@Fuc-PPCD rapidly to release IR783.

In vivo targeted recognition of damaged vascular endothelial cells by PPCD cores

As demonstrated in vitro, the Fuc shell of Fuc-PPCD can be removed under the high shear force at thrombus site. Then LSIPPKA modified PLGA (PPCD) cores were desired to recognize LOX-1 receptor on damaged endothelial cells and to realize sustained release of TI locally. The in vitro targeting ability of PPCD to damaged

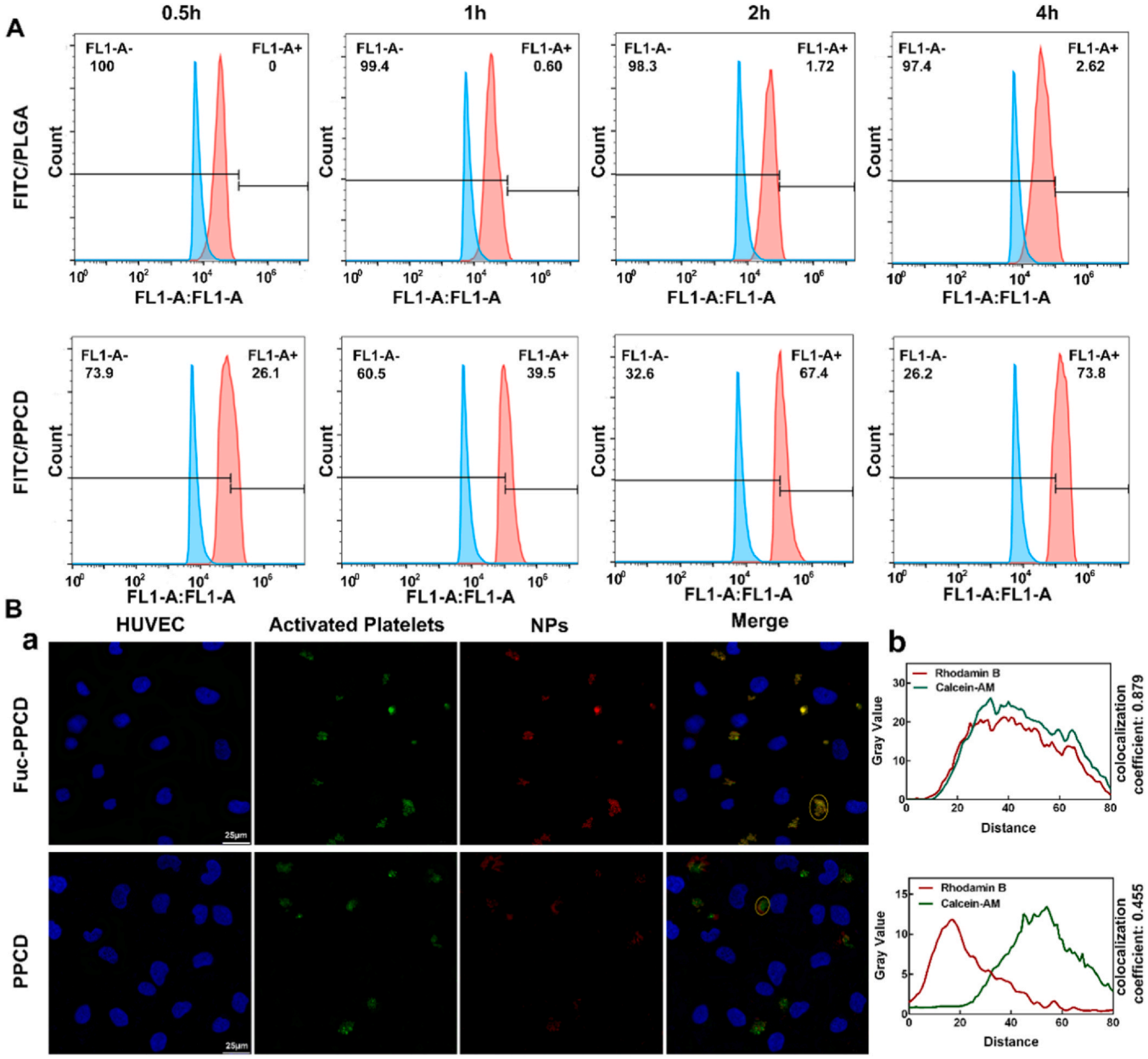

Fig. 5. The targeting mechanism of PPCD and Fuc-PPCD NPs. (A) Flow cytometry analysis to evaluate the targeted ability of PLGA and PPCD NPs to damaged HUVEC cells. NPs were labeled with FITC fluorescent dye. (B) a: Confocal microscopy analysis to evaluate the colocalization ability of Fuc-PPCD NPs with activated platelets. Nuclei of HUVEC cells were stained with Hoechst 33342 (blue), activated platelets were labeled with Calcein-AM (green), while PPCD and Fuc-PPCD were labeled with Rhodamin-B (red). b: the quantitative analysis of colocalization coefficient of NPs and activated platelets. The representative NPs and activated platelets were indicated by a yellow circle.

HUVEC cells had been proved. Herein, the in vivo targeting ability of PPCD to damaged vascular endothelial cells was also evaluated. In order to carry out this experiment, $FeCl_3$ was used to cause vascular injury while without thrombus formation by previously injecting a certain dose of UK into rats. As shown in Fig. 6G and H, after administration for 10 min, there were significantly more IR783@PPCD NPs accumulation in the damaged carotid artery than that of the normal side. And at 30 min, the accumulation of IR783@PPCD NPs in the damaged blood vessel reached the maximum, along with the continuous progress of blood circulation. Thereafter, due to the sustained release of IR783 from PPCD NPs, the fluorescence intensity at the damaged blood vessel gradually decreased. This result further indicated that TI loaded PPCD cores can accurately identify the damaged blood vessels at thrombolysis site, and release TI at fixed point to prevent blood vessel re-embolization after thrombolysis.

In vitro thrombolytic effect

The blood of rats was collected and incubated with thrombin immediately to induce blood clots formation. After that, clots were transferred in a 24-multi-well dish and treated with N.S. (saline), UK,

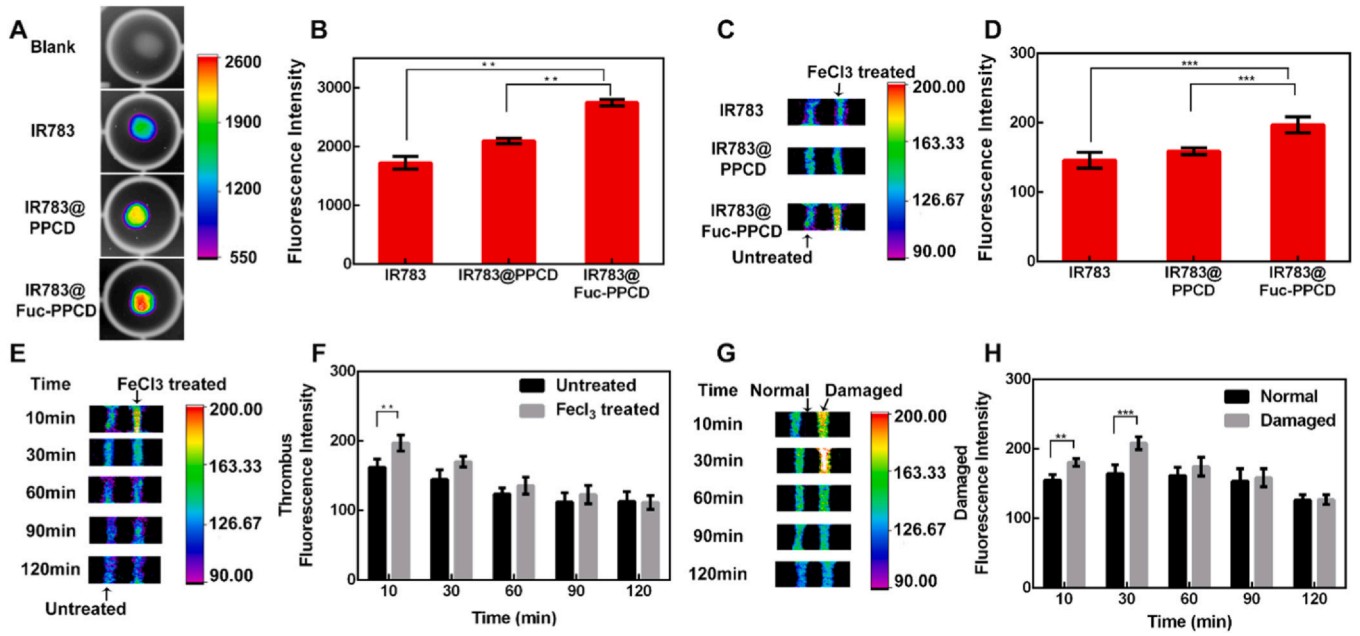

Fig. 6. In vitro and in vivo thrombus targeting study. (A) Representative fluorescence images of in vitro clots treated with IR783, IR783@PPCD and IR783@Fuc-PPCD. (B) Quantitative fluorescence intensity of clots. Data is shown as mean ± SD (n = 3). (C) Representative fluorescence images of bilateral carotid arteries of rats after administration with IR783, IR783@PPCD and IR783@Fuc-PPCD for 10 min (D) Quantitative fluorescence intensity of $FeCl_3$ pre-treated carotid artery in (C). Data is shown as mean ± SD (n = 6). (E) Real-time fluorescence images of bilateral carotid arteries treated with IR783@Fuc-PPCD. (F) Quantitative fluorescence intensity of bilateral carotid arteries in (E). Data is shown as mean ± SD (n = 6). (G) Real-time fluorescence images of normal and damaged carotid arteries treated with IR783@ PPCD NPs. (H) Quantitative fluorescence intensity of normal and damaged vessels in (G). Data is shown as mean ± SD (n = 6). $^{*}p < 0.05$, $^{**}p < 0.01$ and $^{**}p < 0.001$.

TI, TI/PPCD, Fuc-PPCD, UK@Fuc-TI/PPCD and shear stress UK@Fuc-TI/PPCD (pre-shearing in vitro), respectively. Fig. 7A showed representative images of blood clots in different groups after treatment for 0, 1, 2 and 3 h. UK and shear stress UK@Fuc-TI/PPCD groups demonstrated obvious thrombolytic effect, compared with the other groups. TI is an antiplatelet drug, which cannot directly dissolve fibrin in formed thrombus and play a thrombolytic role, thereby no thrombolytic effect was observed in TI group. UK@Fuc-TI/PPCD cannot release UK in a short time without shearing, so it exhibited relatively weak thrombolytic effect. In addition, there was no significant difference in Fuc-PPCD and N.S. control groups, indicating that Fuc-PPCD nanocarriers had no thrombolytic effect. To further investigate the therapeutic efficacy, we compared the thrombus weights and thrombolysis rates of the seven groups. Fig. 7B showed the weight changes of blood clots treated with formulations for different times, and this result was similar to that of images in Fig. 7A. Meanwhile, as Fig. 7C shown, the thrombolytic rates of shear stress UK@Fuc-TI/PPCD and free UK were 91.59% and 100%, respectively.

In vivo thrombolytic effect and the bleeding risk evaluation

After 2 h of administration, carotid artery on the thrombus side was dissected out for H & E staining. As shown in Fig. 7D, the thrombus in N.S. control group completely blocked the blood vessel. In the contrast, the thrombus was almost completely dissolved in UK@Fuc-TI/PPCD group. Meanwhile, the thrombus closure rate of each group was calculated to quantify the thrombolytic effect (Fig. 7E). Compared with 93.10% thrombus closure in N.S. group, Fuc-PPCD nanocarrier (87.30%) did not have significant thrombolytic effects. The pre-shear stress UK@Fuc-TI/PPCD group with the thrombus closure rate of 28.47% showed the similar thrombolytic effects with free UK (26.52%), because UK had been released from UK@Fuc-TI/PPCD after shearing in vitro and played thrombolytic effect as a free drug after entering the body. However, UK@Fuc-TI/PPCD treatment significantly decreased the percentage of thrombus closure, suggesting the great potential in thrombolytic therapy. Moreover, the thrombus closure rates of TI/PPCD, UK@Fuc-PPCD and UK@Fuc-TI/PPCD treatment groups were 50.79%, 18.26% and 9.37%, respectively. This result indicated that compared with UK@Fuc-PPCD group, TI and UK combination group (UK@Fuc-TI/PPCD) can double the efficiency of thrombolysis. This was because that the locally sustained release of TI can effectively prevent the re-embolization of blood vessels after thrombolysis by UK.

In addition, the tail bleeding time of rats treated with different formulations (Fig. 7F) was measured to evaluate the bleeding risk. The bleeding time in UK and UK@Fuc-TI/PPCD groups was 9.96 min and 5.53 min, respectively, proving that UK@Fuc-TI/PPCD can significantly reduce the uncontrollable bleeding risk of UK. This was mainly due to the thrombus targeting and fixed-point drug release characteristics of UK@Fuc-TI/PPCD. What's more, the coagulation index results of rat plasma were shown in Fig. S10. Compared with the saline group, there was no significant difference in blood coagulation parameters, such as APTT (activated partial thromboplastin time), FIB (fibrinogen), PT (prothrombin time) and TT (thrombin time), after treatment with UK@Fuc-TI/PPCD. However, free UK treatment led to significant changes in these parameters, indicating a high risk of bleeding.

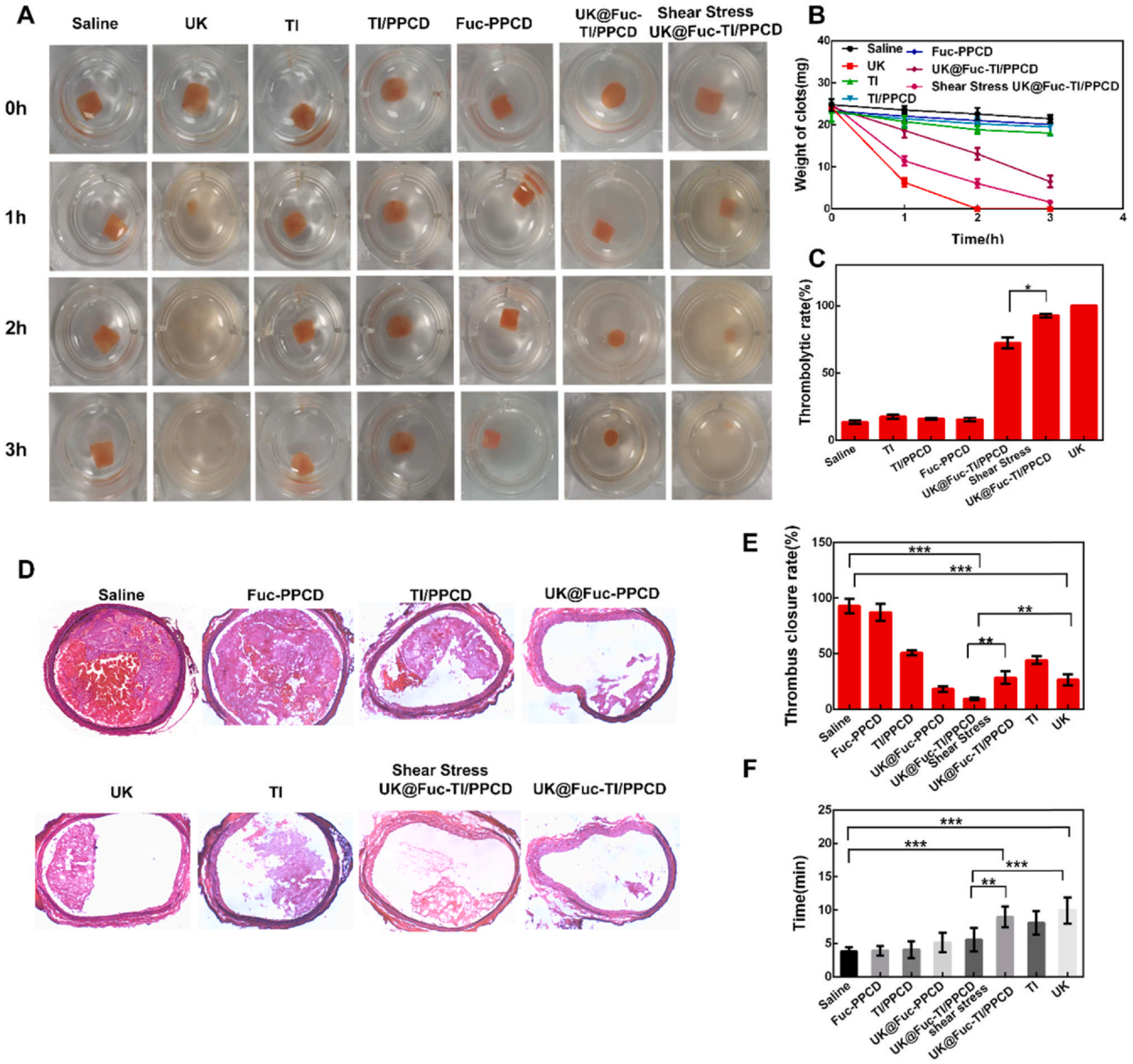

Fig. 7. In vitro and in vivo thrombolytic effect. (A) Representative images of blood clots treated with saline, UK, TI, TI/PPCD, Fuc-PPCD, UK@Fuc-TI/PPCD and shear stress UK@Fuc-TI/PPCD. (B) Weight changes of blood clots treated with different formulations at different time points. Data is shown as mean ± SD (n = 3). (C) Thrombolytic rate of different formulations in vitro. Data is shown as mean ± SD (n = 3). (D) H&E staining results of carotid artery on the thrombus side after 2 h of administration. (E) Thrombus closure rate calculated from images in (D). Data is shown as mean ± SD (n = 6). (F) The tail bleeding time of model rats after administration for 10 min. Data is shown as mean ± SD (n = 6). Notes: Shear Stress UK@Fuc-TI/PPCD indicated that UK@Fuc-TI/PPCD was pre-sheared in vitro for 20 min under the shear force of 1000 dyne/cm^2. $^*p < 0.05$, $^{**}p < 0.01$, $^{***}p < 0.001$.

Biosafety evaluation and in vivo distribution

The healthy SD rats were randomly divided into the following groups: N.S., Fuc-PPCD, UK+TI and UK@Fuc-TI/PPCD. One week after adminstration, main organs were dissected and analyzed by H&E staining. As shown in Fig. 8A, it could be observed that no obvious lesion in UK@Fuc-TI/PPCD group. Meanwhile, there was no significant difference in body weight (Fig. 8B) change within 7 days. In addition, the liver and kidney function indexes of each group were examined and there was no significant difference from the control group (Fig. 8C and D). These results indicated that UK@Fuc-TI/PPCD had good safety in vivo. In vivo distribution result demonstrated this NDDS mainly distribuated in the liver, kidney and lung tissues (Fig. 8E).

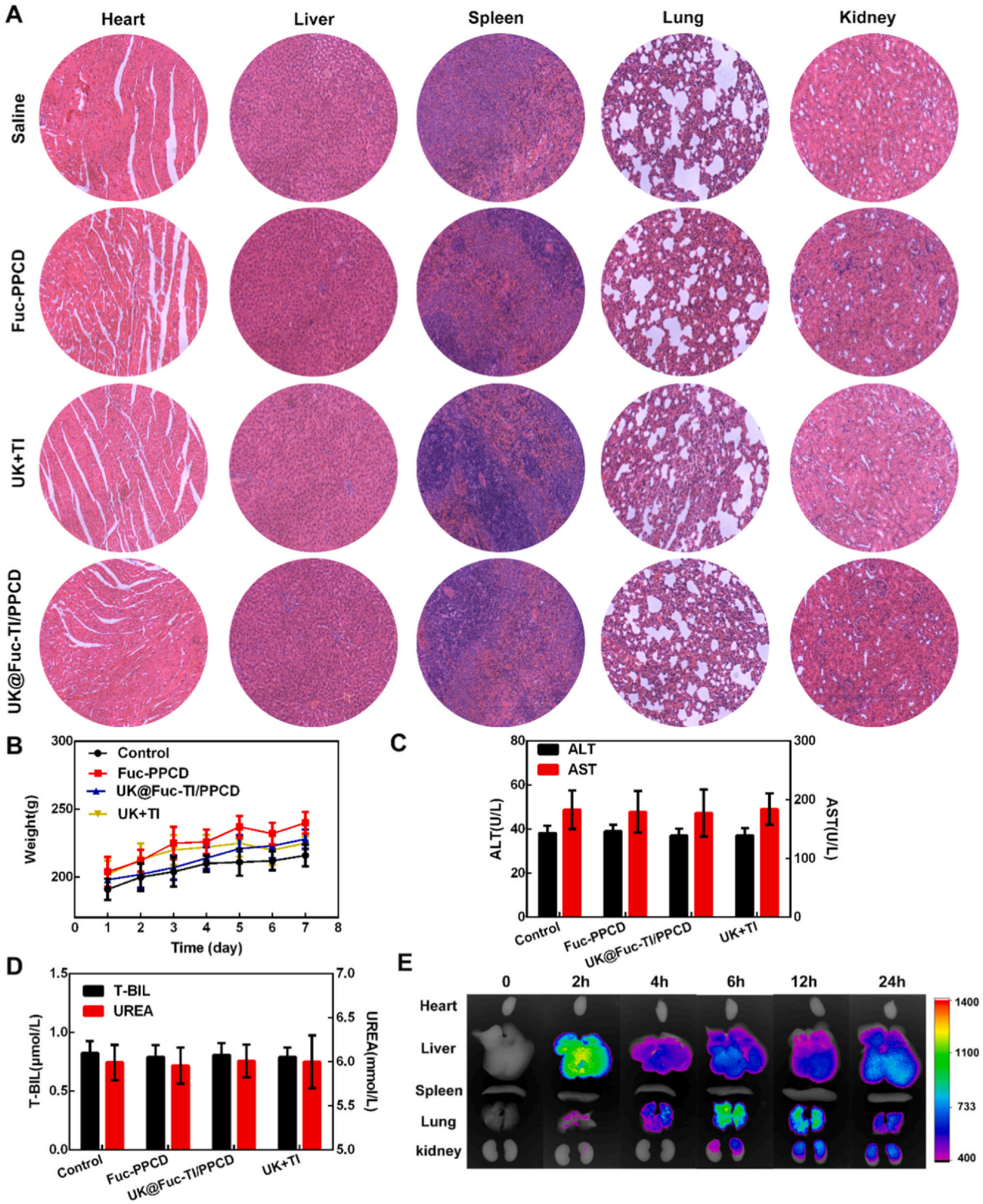

Fig. 8. Biosafety evaluation and in vivo distribution. (A) H&E staining results of main tissues. (B) The body weight changes of rats injected with indicated formulations. Data is shown as mean ± SD (n = 6). (C and D) The liver and kidney function indexes of each group. Data is shown as mean ± SD (n = 6). (E) In vivo distribution of Fuc-PPCD nanocarriers in major tissues at different time points.

Conclusion

In summary, based on the thrombosis microenvironment, this project constructed a shear force responsive and fixed-point separated NDDS (UK@Fuc-TI/PPCD) for "combined attack and defense" treatment of arterial thrombosis. Firstly, UK@Fuc-TI/PPCD can automatically recognize thrombus and achieve precise homing through the binding of Fuc and P-selectin. Then the thrombolytic drug UK and antiplatelet drug TI can be released sequentially on demand, to prevent blood vessel re-embolization after thrombolysis. In vitro and

in vivo results demonstrated UK@Fuc-TI/PPCD NPs had a strong thrombolytic effect and relatively high biosafety. It can significantly improve the recanalization rate of embolized vessels while reduce the uncontrolled bleeding risk synchronously. This study provided a new strategy for the treatment of thrombotic diseases.

CRediT authorship contribution statement

HJ.Z., **L.H.**, and **L.Z.** designed the experiments. **YM.P.**, **LY.G.**, **QQ.H.** and **HL.Z.** were involved in experiments. **HJ.Z.**, **L.H.**, and **ZZ.Z.** analyzed the data and wrote the paper.

Declaration of Competing Interest

The authors declare that they have no known competing financial interests or personal relationships that could have appeared to influence the work reported in this paper.

Acknowledgements

This work was supported by grants from China Postdoctoral Science Foundation Grant (2019M662554), Youth Talent Promotion Project in Henan Province (2020HYTP011), National Natural Science Foundation of China (81874304) and Henan Postdoctoral Research Grant (No. 1902003).

Author Statement

All datasets generated for this study are included in the manuscript and/or the supplementary files.

Appendix A. Supporting information

Supplementary data associated with this article can be found in the online version at doi:10.1016/j.nantod.2021.101186.

References

[1] J. Xu, Y. Zhang, J. Xu, G. Liu, C. Di, X. Zhao, X. Li, Y. Li, N. Pang, C. Yang, Y. Li, B. Li, Z. Lu, M. Wang, K. Dai, R. Yan, S. Li, G. Nie, Engineered nanoplatelets for targeted delivery of plasminogen activators to reverse thrombus in multiple mouse thrombosis models, Adv. Mater. 32 (2019) 1905145.
[2] N. Mackman, Triggers, targets and treatments for thrombosis, Nature 451 (2008) 914–918.
[3] E. Yilmazel, Ucar, Eurasia J. Med. 51 (2019) 185–189.
[4] M. Stefanovic Budimkic, T. Pekmezovic, L. Beslac-Bumbasirevic, M. Ercegovac, I. Berisavac, P. Stanarcevic, V. Padjen, D.R. Jovanović, Long-term prognosis in ischemic stroke patients treated with intravenous thrombolytic therapy, J. Stroke Cerebrovasc. Dis. 26 (2017) 196–203.
[5] T. Huang, N. Li, J. Gao, Recent strategies on targeted delivery of thrombolytics, Asian J. Pharm. Sci. 14 (2019) 233–247.
[6] E. Jung, C. Kang, J. Lee, D. Yoo, D.W. Hwang, D. Kim, S.-C. Park, S.K. Lim, C. Song, D. Lee, Molecularly engineered theranostic nanoparticles for thrombosed vessels: H_2O_2-activatable contrast-enhanced photoacoustic imaging and antithrombotic therapy, ACS Nano 12 (2018) 392–401.
[7] C. Li, H. Du, A. Yang, S. Jiang, Z. Li, D. Li, J.L. Brash, H. Chen, Thrombosis-responsive thrombolytic coating based on thrombin-degradable tissue plasminogen activator (t-PA) nanocapsules, Adv. Funct. Mater. 27 (2017) 1703934.
[8] M.K. Netanel Korin, B.D. Matthews, M. Crescente, A. Brill, T. Mammoto, K. Ghosh, S. Jurek, S.A. Bencherif, A.U.C. Deen Bhatta, C.L. Feldman, D.D. Wagner, D.E. Ingber, Shear-activated nanotherapeutics for drug targeting to obstructed blood vessels, Science 337 (2012) 738–742.
[9] D.L. Bark, D.N. Ku, Wall shear over high degree stenoses pertinent to atherothrombosis, J. Biomech. 43 (2010) 2970–2977.
[10] C.P. Molloy, Y. Yao, H. Kammoun, T. Bonnard, T. Hoefer, K. Alt, F. Tovar-Lopez, G. Rosengarten, P.A. Ramsland, A.D. van der Meer, A. van den Berg, A.J. Murphy, C.E. Hagemeyer, K. Peter, E. Westein, Shear-sensitive nanocapsule drug release for site-specific inhibition of occlusive thrombus formation, J. Thromb. Haemost. 15 (2017) 972–982.
[11] M.N. Holme, I.A. Fedotenko, D. Abegg, J. Althaus, L. Babel, F. Favarger, R. Reiter, R. Tanasescu, P.-L. Zaffalon, A. Ziegler, B. Müller, T. Saxer, A. Zumbuehl, Shear-stress sensitive lenticular vesicles for targeted drug delivery, Nat. Nanotechnol. 7 (2012) 536–543.
[12] Y.-G. Jia, X.X. Zhu, Chem. Mater. 27 (2014) 387–393.
[13] S. Himmelein, V. Lewe, M.C.A. Stuart, B.J. Ravoo, A carbohydrate-based hydrogel containing vesicles as responsive non-covalent cross-linkers, Chem. Sci. 5 (2014) 1054.
[14] J.A. Kaplan, P. Barthélémy, M.W. Grinstaff, Self-assembled nanofiber hydrogels for mechanoresponsive therapeutic anti-TNFα antibody delivery, Chem. Commun. 52 (2016) 5860–5863.
[15] S.R. Panicker, P. Mehta-D'souza, N. Zhang, A.G. Klopocki, B. Shao, R.P. McEver, Circulating soluble P-selectin must dimerize to promote inflammation and coagulation in mice, Blood 130 (2017) 181–191.
[16] B. Li, R. Aid-Launais, M.-N. Labour, A. Zenych, M. Juenet, C. Choqueux, V. Ollivier, O. Couture, D. Letourneur, C. Chauvierre, Functionalized polymer microbubbles as new molecular ultrasound contrast agent to target P-selectin in thrombus, Biomaterials 194 (2019) 139–150.
[17] M. Juenet, R. Aid-Launais, B. Li, A. Berger, J. Aerts, V. Ollivier, A. Nicoletti, D. Letourneur, C. Chauvierre, Thrombolytic therapy based on fucoidan-functionalized polymer nanoparticles targeting P-selectin, Biomaterials 156 (2018) 204–216.
[18] S.M. Zinkstok, Y.B. Roos, Early administration of aspirin in patients treated with alteplase for acute ischaemic stroke: a randomised controlled trial, Lancet 380 (2012) 731–737.
[19] C. Kleinschnitz, S. Amaro, L. Llull, X. Urra, V. Obach, Á. Cervera, Á. Chamorro, Risks and benefits of early antithrombotic therapy after thrombolytic treatment in patients with acute stroke, PLoS One 8 (2013) e71132.
[20] O. Adeoye, H. Sucharew, J. Khoury, A. Vagal, P.A. Schmit, I. Ewing, S.R. Levine, S. Demel, B. Eckerle, B. Katz, D. Kleindorfer, B. Stettler, D. Woo, P. Khatri, J.P. Broderick, A.M. Pancioli, Combined approach to lysis utilizing eptifibatide and recombinant tissue-type plasminogen activator in acute ischemic stroke-full dose Regimen Stroke Trial, Stroke 46 (2015) 2529–2533.
[21] L.E.I. Feng, J.U.N. Liu, Y. Liu, J. Chen, C. Su, C. Lv, Y. Wei, Exp. Ther. Med. 11 (2016) 1011–1016.
[22] W. Hu, Q. Xie, H. Xiang, Impact of elevated circulating histones on systemic inflammation after radiofrequency ablation in lung cancer patients, BioMed. Res. Int. 2017 (2017) 1–6.
[23] H. Gao, Y.-w Yang, Y.-g Fan, J.-b Ma, Conjugates of poly(DL-lactic acid) with ethylenediamino or diethylenetriamino bridged bis(beta-cyclodextrin)s and their nanoparticles as protein delivery systems, J. Control. Release 112 (2006) 301–311.
[24] H. Gao, Y.-N. Wang, Y.-G. Fan, J.-B. Ma, Conjugates of poly(DL-lactide-co-glycolide) on amino cyclodextrins and their nanoparticles as protein delivery system, J. Biomed. Mater. Res. Part A 80A (2007) 111–122.
[25] J. Zhang, H. Zhang, R. Xu, Solubility determination and modeling for tirofiban in several mixed solvents at 278.15–323.15 K, J. Chem. Eng. Data 65 (2020) 4071–4078.
[26] R.I. El-Bagary, E.F. Elkady, N.A. Farid, N.F. Youssef, Validated spectrofluorimetric methods for the determination of apixaban and tirofiban hydrochloride in pharmaceutical formulations, Spectrochim. Acta Part A Mol. Biomol. Spectrosc. 174 (2017) 326–330.
[27] E. Westein, A.D. van der Meer, M.J.E. Kuijpers, J.-P. Frimat, A. van den Berg, J.W.M. Heemskerk, Atherosclerotic geometries exacerbate pathological thrombus formation poststenosis in a von Willebrand factor-dependent manner, Proc. Natl. Acad. Sci. USA 110 (2013) 1357–1362.
[28] X. Zhou, L. Chen, A. Wang, Y. Ma, H. Zhang, Y. Zhu, Multifunctional fluorescent magnetic nanoparticles for lung cancer stem cells research, Colloids Surf. B Biointerfaces 134 (2015) 431–439.
[29] J. Li, L. Zheng, H. Cai, W. Sun, M. Shen, G. Zhang, X. Shi, Polyethyleneimine-mediated synthesis of folic acid-targeted iron oxide nanoparticles for in vivo tumor MR imaging, Biomaterials 34 (2013) 8382–8392.
[30] S.J. White, S.A. Nicklin, T. Sawamura, A.H. Baker, Identification of peptides that target the endothelial cell-specific LOX-1 receptor, Hypertension 37 (2001) 449–455.
[31] M. Bortot, K. Ashworth, A. Sharifi, F. Walker, N.C. Crawford, K.B. Neeves, D. Bark, J. Di Paola, Arteriosclerosis, Thromb., Vasc. Biol. 39 (2019) 1831–1842.